International Journal of Advanced Engineering, Management and Science (IJAEMS)
Peer-Reviewed Journal
ISSN: 2454-1311 | Vol-12, Issue-2; Mar-Apr, 2026
Journal Home Page: https://ijaems.com/
DOI: https://dx.doi.org/10.22161/ijaems.122.9

Fuzzy PID Intelligent Control of System Model

Hung Yu Chen[1], Zi Xian Huang[2], Ming Hui Huang[3], Zou Zheng Hao Dong[4], Ho Sheng Chen[5*]

[1]Guangzhou Institute of Science and Technology, China
Email: ronwisely@outlook.com
[2,3,4,5]School of Sciences, Guangdong University of Petrochem Technology (GDUPT), Maoming 525000, China
Corresponding author: Ho-Sheng Chen
Email: hschen98.tw@gmail.com

Received: 13Feb 2026; Received in revised form: 12 Mar 2026; Accepted:17 Mar 2026; Available online: 21 Mar 2026

Abstract— *To improve the control performance of conventional PID controllers in nonlinear and time-varying uncertain systems, a fuzzy neural network PID control algorithm is proposed. This approach integrates the nonlinear control advantages of fuzzy logic with the self-learning and adaptive characteristics of neural networks to achieve real-time online tuning of PID parameters. Based on the mathematical model of an electro-hydraulic servo control system, a fuzzy neural network PID control system model is developed. Taking the control system of a transplanting manipulator as a case study, simulations are conducted using Matlab/Simulink, with the transfer function of the electro-hydraulic servo control system serving as the controlled object. The tracking performance of different control systems is evaluated by comparing traditional PID control, Type-1 fuzzy PID control, interval Type-2 fuzzy PID control, and fuzzy neural network PID control methods employing various membership functions. Simulation and experimental results demonstrate that the fuzzy neural network PID controller exhibits superior control performance compared to traditional PID control, Type-1 fuzzy PID control, and interval Type-2 fuzzy PID control in the target system.*

Keywords— ***fuzzy neural network; PID control; electro-hydraulic servo system; transplanting manipulator; Matlab/Simulink simulation***

I. INTRODUCTION

the introduction of the paper should explain the nature of the problem, previous work, purpose, and the contribution of the paper. The contents of each section may be provided to understand easily about the paper.

At present, electro-hydraulic servo system is widely used in industrial production and aerospace [1]. In fields such as mechanical manufacturing, this technology employs a combined electric-hydraulic approach to achieve precise motion control. As a primary method for high-performance closed-loop control in hydraulic systems, its core mechanism involves motor-driven oil pumps that draw hydraulic fluid into pipelines. Electronic signals from the controller regulate hydraulic valves, which then direct the fluid to actuators like cylinders or motors. The fluid entering the cylinder pushes pistons to drive load movement [2]. It has the characteristics of high power-to-weight ratio, fast response, high stiffness and low maintenance cost. The characteristics of fast response of electrical system and high output power of hydraulic system can be reflected in the electro-hydraulic servo system [3]. In the control of electro-hydraulic servo systems, widely used PID control is relatively easy to implement and can achieve good results. However, conventional PID controllers lack adaptive parameter adjustment capabilities. When dealing with nonlinear and time-varying uncertain electro-hydraulic servo systems, there remains room for optimization and improvement. This necessitates enhancing control performance beyond the basic PID controller framework [4,5].

To investigate which control scheme is superior when compared with conventional PID controllers, Type 1 fuzzy PID controllers, interval-type Type 2 fuzzy PID controllers, and fuzzy neural network PID controllers in handling uncertain nonlinear time-varying systems, we will select an uncertain nonlinear time-varying system as the control object. Given the widespread application of electro-hydraulic servo systems, they serve as a representative example of such nonlinear time-varying systems. Jin X., Chen K., Zhao Y., et al. have previously developed simulation models for transplanting robotic arms in their research. The transplanting robotic arm employs a hydraulic control system featuring an electro-hydraulic servo valve. A mathematical model was developed to simulate fuzzy PID control, validating the feasibility of applying this controller to robotic arm operations. Building upon the transfer function of the controlled system, four controller designs were developed using fuzzy control theory and automatic control principles: conventional PID controller, Type 1 fuzzy PID controller, interval-type Type 2 fuzzy PID controller, and a fuzzy neural network PID controller [7-10].

II. SYSTEM DESCRIPTION

The electro-hydraulic servo system operates on Pascal's law. It is primarily categorized into valve-controlled and pump-controlled types, both sharing similar control logic for regulating output position, force, or speed. This study focuses on the valve-controlled system, as illustrated in Fig. 1, specifically designed to control the position output of the hydraulic cylinder piston.

The power source for electro-hydraulic servo systems typically originates from the hydraulic pump at the actuators front end, which generates pressure differentials in the fluid through high-speed operation. Displacement sensors and pressure sensors respectively transmit position signals from the end effector and hydraulic pressure signals back to the controller. The controller then outputs servo electrical signals to the electro-hydraulic servo valve via a servo amplifier, thereby controlling the end effector as illustrated in Fig. 2.

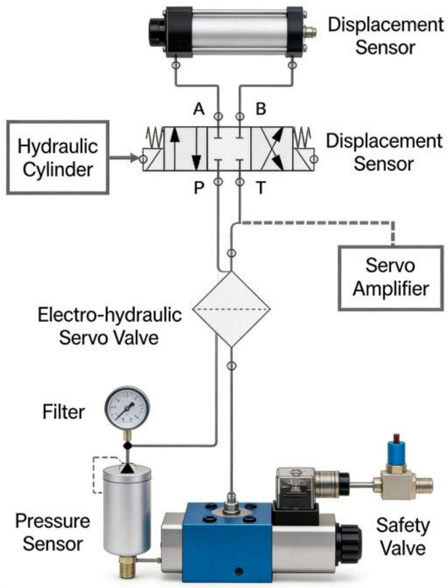

Fig.1. Valve controlled electro-hydraulic servo system diagram

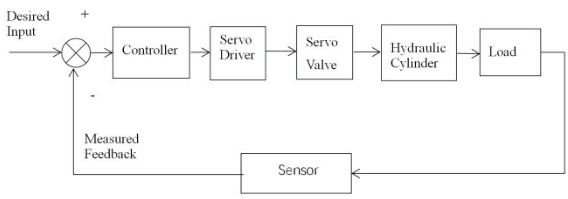

Fig.2. Closed-loop control block diagram of electro-hydraulic servo system

The power source of an electro-hydraulic servo system is usually the hydraulic pump at the front end, which creates pressure increase in the fluid through the high-speed operation of the pump. The position signal and liquid pressure signal of the end effector are fed back to the controller using displacement sensors and pressure sensors, respectively. Finally, the controller outputs the servo electrical signal to the electro-hydraulic servo valve through a servo amplifier to control the end effector. In addition, the control of the electro-hydraulic servo control system is also affected by the flow of liquid between the valve port, valve, and hydraulic cylinder, as well as the load on the hydraulic cylinder itself during work. Therefore, the three fundamental time-domain equations of the electro-hydraulic servo system are given, the valve port flow equation:

$$q_L = K_q x_v - K_c p_L \quad (1)$$

The continuity equation of hydraulic cylinder flow:

$$q_{\mathrm{L}} = A_{\mathrm{p}}\frac{\mathrm{d}x_{\mathrm{p}}}{\mathrm{d}t} + C_{\mathrm{tp}}p_{\mathrm{L}} + \frac{V_{\mathrm{t}}}{4\beta_{\mathrm{e}}}\frac{\mathrm{d}p_{\mathrm{L}}}{\mathrm{d}t} \quad (2)$$

The force balance equation of hydraulic cylinder:

$$A_{\mathrm{p}}p_{\mathrm{L}} = m_{\mathrm{t}}\frac{\mathrm{d}^2x_{\mathrm{p}}}{\mathrm{d}t^2} + B_{\mathrm{p}}\frac{\mathrm{d}x_{\mathrm{p}}}{\mathrm{d}t} + Kx_{\mathrm{p}} + F_{\mathrm{L}} \quad (3)$$

After applying the Laplace transform to the three major time-domain equations mentioned above, we obtain the three fundamental frequency-domain equations of the electro-hydraulic servo system:

Valve port flow equation:

$$Q_L = K_q X_V - K_c P_L \quad (4)$$

where Q_L represents the flow rate through the load, K_q is the servo valve flow gain, X_V is the effective spool displacement, K_c is the servo valve flow pressure gain, and P_L is the load pressure

The continuity equation of hydraulic cylinder flow:

$$Q_L = A_p sX_p + C_{tp}P_L + \frac{V_t}{4\beta_e}sP_L \quad (5)$$

Where A_p is the effective area of the hydraulic piston during operation, X_p is the piston displacement during operation, C_{tp} is the total leakage coefficient of the hydraulic cylinder, β_e is the effective bulk modulus of the oil, and V_t is the total volume of the two chambers of the hydraulic cylinder.

The force balance equation of hydraulic cylinder:

$$A_pP_L = m_ts^2X_p + B_psX_p + KX_p + F_L \quad (6)$$

Considering the terminal load as a variable load composed of mass, spring, and damping, which includes three parts: inertia, elasticity, and damping. Without considering the influence of external load forces, the force balance equation of the hydraulic cylinder can be obtained based on Newton's second law and where m_t is the equivalent load mass, B_p is the load viscous friction coefficient, K is the load elastic coefficient, and F_L is the force acting on the piston rod of the hydraulic cylinder. Based on the effective spool displacement X_V in the above three fundamental frequency domain equations and the piston displacement X_p during operation, the open-loop transfer function of the system is obtained as follows:

$$\mathrm{G(s)} = \frac{\mathrm{X_p}}{X_{\mathrm{v}}} = \frac{\dfrac{K_{\mathrm{q}}}{A_1}}{s\left(\dfrac{s^2}{\omega_{\mathrm{h}}^2} + \dfrac{2\zeta_{\mathrm{h}}}{\omega_{\mathrm{h}}}s + 1\right)} \quad (7)$$

where A_1 represents the equivalent working area of the hydraulic cylinder piston rod during displacement, ζ_{h} denotes the damping ratio of the hydraulic cylinder, and ω_{h} signifies the natural frequency of the hydraulic cylinder. The natural frequency ω_{h} can be calculated as follows:

$$\omega_h = \sqrt{\frac{4\beta_e A_P^2}{V_t m_t}} \quad (8)$$

The damping ratio ζ_{h} can be calculated as follows:

$$\zeta_h = K_{ce}\sqrt{\frac{m_t\beta_e}{V_tA_p^2}} + \frac{B_P}{4}\sqrt{\frac{V_t}{m_t\beta_eA_P^2}} \quad (9)$$

The closed-loop transfer function can be obtained

$$\phi(S) = \frac{G(s)}{1+G(s)} = \frac{K_v}{\left(\dfrac{s^3}{\omega_h^2} + \dfrac{2\zeta_h}{\omega_h}s^2 + s + K_v\right)} \quad (10)$$

The structure of the transplanting robotic arm is shown in the Fig. 3, where 1. Conductive liquid injection hole, 2. Hydraulic pump, 3. Power output shaft, 4. Rotating power output bracket, 5. Clamp jaw fixing device, 6. Oil pipeline outlet, 7. Clamp jaw, 8. Spring, 9. Clamping device, and 10. Rotating sleeve, respectively.

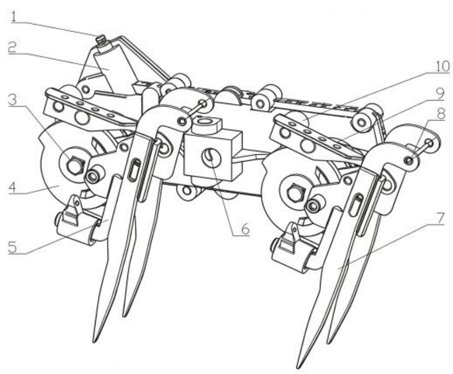

Fig.3. The ransplanting robot structure

Jin X, Chen K, Zhao Y, et al. constructed a simulation model for a transplanting robotic arm in their research [11]. The robotic arm employed hydraulic control incorporating an electro-hydraulic servo valve, and the obtained mathematical model was utilized to complete the simulation of fuzzy PID control. Therefore, this paper refers to the simulation configuration parameters introduced by Jin X, Chen K, Zhao Y, et al. in their article for data calculation. As shown in Table 1.

Table. 1. Simulation parameters of electro-hydraulic servo system [11]

variable	value	variable	value
Q_L	209	m	0.24
K_q	5	F_L	$11e^4$
C_{tp}	$1.5e^{-10}$	β_e	$7e^8$
V_t	$5.8e^{-5}$	A_p	$4.4e^{-3}$
B_P	$2e^5$	K_h	$2.5e^7$
ω_m	185	K_f	$2.5e^{-5}$

Ultimately, the closed-loop transfer function of the control object can be obtained

$$G(s) = \frac{208.75}{s^3 + 14.31s^2 + 447.53s + 208.75} \quad (11)$$

III. CONTROLLER DESIGN

PID controllers are widely used in modern control fields due to their simple structure and ease of implementation. Before designing a PID controller, we must first clarify its components: a conventional PID controller mainly consists of three parts: proportional, integral, and derivative. Based on this, we obtain the closed-loop system transfer function in Eq. 11, and the time-continuous equation of the PID controller can be obtained

$$G(s) = \frac{U(s)}{E(s)} = K_p\left(1 + \frac{1}{K_I s} + K_D s\right) \quad (12)$$

where K_p, K_I, and K_D represent the proportional coefficient, integral time (also known as integral coefficient), and derivative time (also known as derivative coefficient) of the controller, respectively. These components adjust the output signal by monitoring the error between the feedback signal and the set value, ensuring that the system response reaches the desired value. The design of a Type-1 fuzzy PID controller (T1FPID) is used to enable the controlled system to track the target signal. It can be seen that the overall structure of the controller consists of a Type-1 fuzzy controller, a PID controller, and a controlled object electro-hydraulic servo system, in addition to a feedback loop.

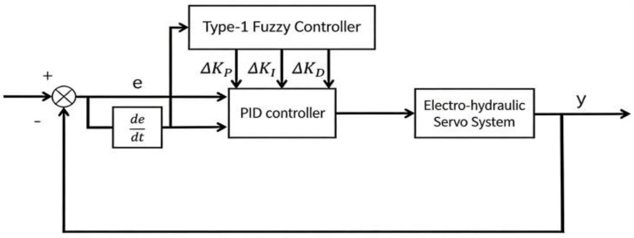

Fig. 4. Structure diagram of type 1-fuzzy PID controller

The structure of the Type 1 fuzzy controller is illustrated in Fig. 5 below, primarily consisting of three main components: fuzzification, fuzzy inference, and defuzzification. From the perspective of input and output signal forms, the fuzzy controller of this system is of the multi-input multi-output type. Its complete design process can be mainly divided into steps such as determining fuzzy variables, establishing the range of the universe of discourse, discretization, fuzzification, establishing fuzzy rules, and defuzzification output. Each step will be introduced and analyzed separately below.

From Fig. 4, we can see that the input of the Type 1 fuzzy controller consists of two parts: the system error e and the rate of change of error de/dt (hereinafter defined as ec). The output consists of three parts: ΔK_P, ΔK_I, and ΔK_D. Therefore, we have determined the variables involved in the fuzzification process in this controller.

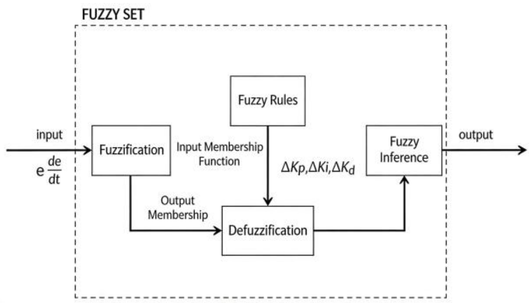

Fig.5: Structure of Type-1 Fuzzy Controller

Compared to the aforementioned Type-1 fuzzy PID controller, the structure of the Interval Type-2 fuzzy PID controller is identical, as illustrated in Fig. 6. It can be observed that the overall structure of the controller consists of an Interval Type-2 fuzzy controller, a PID controller, and the controlled object, which is an electro-hydraulic servo system.

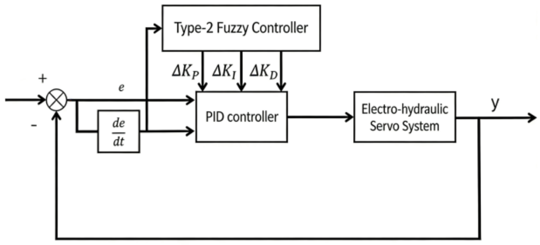

Fig. 6. Structure diagram of type 2-fuzzy PID controller

In the representation of fuzzy sets, the Type-1 fuzzy controller employs a fixed-shape membership function to represent fuzzy sets. It handles system uncertainties through fuzzy logic and fuzzy inference, but may perform inadequately when faced with significant uncertainties. In the Interval Type-2 fuzzy controller, fuzzy sets are represented using intervals, meaning the fuzzy set for each input variable is represented as an interval rather than a specific membership function. This approach enables better handling of system uncertainties, as intervals can describe uncertainties within a certain range. In the design presented in this section, the interval representation of fuzzy sets in the Interval Type-2 fuzzy controller is formed by shifting the membership function of the Type-1 fuzzy controller, representing an extended form of the Type-1 fuzzy controller's membership function. Its functional characteristics are based on the Gaussian membership function. To understand the fuzzy sets in the interval type-2 fuzzy controller, we can assume that we have two Gaussian functions, denoted as $G_1(x)$ and $G_2(x)$, respectively. Their mathematical expressions are as follows:

$$G_1(x) = \frac{1}{\sigma_1\sqrt{2\pi}} e^{-\frac{(x-\mu_1)^2}{2\sigma_1^2}} \tag{13}$$

$$G_2(x) = \frac{1}{\sigma_2\sqrt{2\pi}} e^{-\frac{(x-\mu_2)^2}{2\sigma_2^2}} \tag{14}$$

where σ_i, μ_i, i=1, 2, represents the standard deviation of the corresponding Gaussian function and the mean of the corresponding Gaussian function, respectively. The shape of the Gaussian function will change with the change of the mean and standard deviation. As shown in Fig. 7, the interval type-2 Gaussian membership function, the standard deviation and mean of the two Gaussian functions are as follows:

$$\sigma_1 = 0.7078, \quad \sigma_2 = 0.56624, \quad \mu_1 = 2, \quad \mu_2 = 2.$$

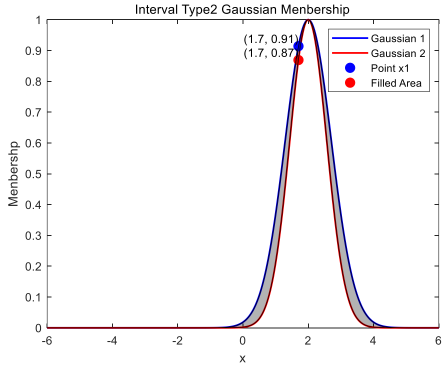

Fig. 7. Calculation of interval Type-2 Gaussian membership function

After summing $G_1(x)$ and $G_2(x)$ and taking their average, the resulting arithmetic mean is the actual membership function. Substituting x_0=1.7 into Eq. (13) and (14), we obtain $G_1(x)$ =0.91 ； $G_2(x)$ =0.87. Therefore, the actual membership degree at the point x_0=1.7 is:

$$G_f(x) = \frac{G_1(x) + G_2(x)}{2} = \frac{0.91 + 0.87}{2} = 0.89 \tag{15}$$

Similarly, after determining the mathematical expression of the membership function, it is necessary to establish the fuzzy domains for the controller's input and output. The interval type-2 fuzzy controller has two inputs and three outputs, making it a multi-input multi-output system. The inputs to the interval type-2 fuzzy controller include the system error e and the rate of change of error ec. The outputs of the interval type-2 fuzzy controller include ΔK_P, ΔK_I, and ΔK_D. Next, the domain ranges for the system error e and the rate of change of error ec are set, both of which are [-6,6]. Subsequently, the domains for ΔK_P, ΔK_I, and ΔK_D are set to [1,3], [1,3], and [0.5,2], respectively, as Fig. 8.

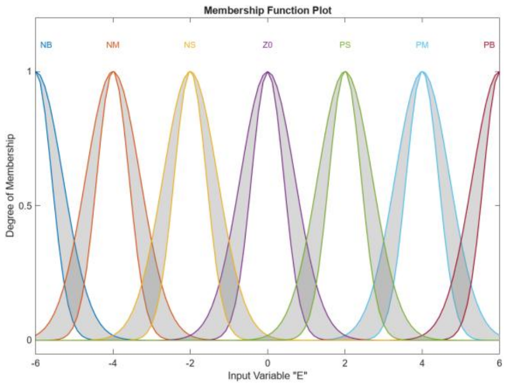

Fig. 8. Membership function of Interval Type2-Fuzzy PID

IV. SIMULATION

To simulate the system model, we constructed systems such as conventional PID control, Type-1 fuzzy PID control, and interval Type-2 fuzzy PID control in the Simulink simulation environment of Matlab according to the controller design content. In addition, to explore the signal tracking capabilities of conventional PID control, Type-1 fuzzy PID control, and interval Type-2 fuzzy PID control, we designed input step signals with variations. Firstly, to facilitate the analysis and comparison of the control capabilities of the three control systems, we integrated them into the same simulation environment as shown in Fig. 9, Simulation of Multiple Controllers in Simulink.

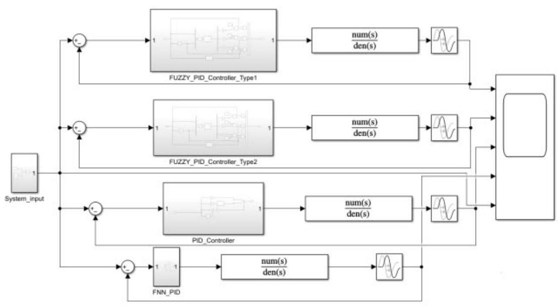

Fig. 9. Simulation of multiple controllers in Simulink

The initial value of the input signal is Position=1.8mm. When the simulation progresses to time=7s, the signal undergoes a step pull-up, raising the target signal value to Position=3mm. After a duration of 2s, at simulation time time=9s, the signal is pulled back to the initial position of 1.8. The signal tracking performance of each controller is observed, and the simulation effect of the system is shown in Fig. 10, which illustrates the simulation effects of various controllers.

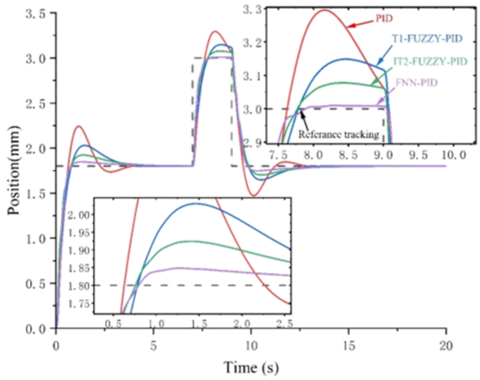

Fig. 10. Output response curve diagram of multiple controllers

V. CONCLUSION

This paper proposes a control strategy based on a fuzzy neural network PID algorithm for real-time dynamic tuning of PID parameters in system models characterized by time-varying uncertainties and nonlinearities. The proposed method integrates the advantages of both fuzzy control and neural networks. The fuzzy controller leverages existing expert experience to accelerate the initialization and learning process of the neural network, while the neural network enhances the self-learning and adaptive capabilities of the fuzzy controller, enabling real-time online tuning of PID parameters. To address the issue of low output precision in transplanting manipulators caused by external disturbances, a mathematical model of a fuzzy neural network PID control system is developed based on a conventional PID controller. Simulation analysis is conducted using Matlab and Simulink. By comparing the control performance of conventional PID control, type-1 fuzzy PID control, interval type-2 fuzzy PID control, and the proposed fuzzy neural network PID control, the results demonstrate the relative superiority of the fuzzy neural network intelligent control strategy for the target system model.

ACKNOWLEDGEMENTS

This research was supported by "Guangdong Scienceand Technology Program", "Research on Investigation ofthe Multimodal Intelligent Flying Electric Motorcycle's Autonomous Motion. (NO.

2024A0505050019)", theirhelp in teaching the research.

REFERENCES

[1] Alimhillaj, P., Lamani, L., & Vedova, D. L. D. M. (2024). Simulation of an aerospace electrohydraulic servomechanism with different Coulomb friction models. *Journal of Physics: Conference Series*, 2716(1).

[2] Mintsa, A. H., Eny, E. G., Senouveau, N., et al. (2023). Optimal tuning PID controller gains from Ziegler-Nichols approach for an electrohydraulic servo system. *Journal of Engineering Research and Reports*, 25(11), 158-166.

[3] Borase, R. P., Maghade, D. K., Sondkar, S. Y., et al. (2021). A review of PID control, tuning methods and applications. *International Journal of Dynamics and Control*, 9, 818-827.

[4] Carvajal, J., Chen, G., & Ogmen, H. (2000). Fuzzy PID controller: Design, performance evaluation, and stability analysis. *Information Sciences*, 123(3-4), 249-270.

[5] Nguyen, A. T., Taniguchi, T., Eciolaza, L., et al. (2019). Fuzzy control systems: Past, present and future. *IEEE Computational Intelligence Magazine*, 14(1), 56-68.

[6] Xiaolin, D., Pengfei, Z., Wanlu, Z., et al. (2023). Fuzzy adaptive PID speed controller design for modern elevator traction machine. *Energy Reports*, 9(S8), 175-183.

[7] Jin, X., Chen, K., Zhao, Y., et al. (2020). Simulation of hydraulic transplanting robot control system based on fuzzy PID controller. *Measurement*, 164.

[8] Castillo, O., & Melin, P. (2012). A review on the design and optimization of interval type-2 fuzzy controllers. *Applied Soft Computing Journal*, 12(4), 1267-1278.

[9] Wu, D., & Mendel, J. M. (2011). On the continuity of type-1 and interval type-2 fuzzy logic systems. *IEEE Transactions on Fuzzy Systems*, 19(1), 179-192.

[10] Li, M., Li, J., Li, G., et al. (2022). Analysis of active suspension control based on improved fuzzy neural network PID. *World Electric Vehicle Journal*, 13(12), 226.

[11] Jin X ,Chen K ,Zhao Y , et al. Simulation of hydraulic transplanting robot control system based on fuzzy PID controller [J]. Measurement, 2020, 164 (prepublish)